



Data Article

Beyond binary parcellation of the vestibular cortex – A dataset



V. Kirsch^{a,b,c,*}, R. Boegle^{b,c,1}, D. Keeser^{d,e}, E. Kierig^{a,c},
B. Ertl-Wagner^{c,d,g}, T. Brandt^{c,f}, M. Dieterich^{a,b,c,g}

^a Department of Neurology, Ludwig-Maximilians Universität, Munich, Germany

^b Graduate School of Systemic Neuroscience, Ludwig-Maximilians Universität, Munich, Germany

^c German Center for Vertigo and Balance Disorders-IFBLMU, Ludwig-Maximilians Universität, Munich, Germany

^d Department of Radiology, Ludwig-Maximilians Universität, Munich, Germany

^e Department of Psychiatry, Ludwig-Maximilians Universität, Munich, Germany

^f Clinical Neuroscience, Ludwig-Maximilians Universität, Munich, Germany

^g Munich Cluster for Systems Neurology (SyNergy), Munich, Germany

ARTICLE INFO

Article history:

Received 8 May 2018

Received in revised form

1 January 2019

Accepted 7 January 2019

ABSTRACT

The data-set presented in this data article is supplementary to the original publication, [doi:10.1016/j.neuroimage.2018.05.018](https://doi.org/10.1016/j.neuroimage.2018.05.018) (Kirsch et al., 2018). Named article describes handedness-dependent organizational patterns of functional subunits within the human vestibular cortical network that were revealed by functional magnetic resonance imaging (fMRI) connectivity parcellation. 60 healthy volunteers (30 left-handed and 30 right-handed) were examined on a 3T MR scanner using resting state fMRI. The multisensory (non-binary) nature of the human (vestibular) cortex was addressed by using masked binary and non-binary variations of independent

DOI of original article: <https://doi.org/10.1016/j.neuroimage.2018.05.018>

Abbreviations: A1, Primary auditory cortex; ACC, Anterior cingulate cortex; BA, Brodmann area; C, Common cluster; CSF, Cerebrospinal fluid; fCBP, Functional connectivity based parcellation; IC, Independent component; ICA, Independent component analysis; IPL, Inferior parietal lobule; L, Left; LH, Left-handed; L-I, Laterality-index; M1, Primary motor cortex; MR, Magnetic resonance; MRI, Magnetic resonance imaging; MST, Medial superior temporal area; MSTd, Dorsal medial superior temporal area; M/STG, Middle and superior temporal gyrus; MT, Middle temporal area; OP, Operculum; OP2, Operculum 2; P, Parcel; P-P, Parcel to parcel correlation; P-RSN, Parcel to resting state network correlation; PET, Positron emission tomography; PIVC, Parieto-insular vestibular cortex; R, Right; RH, Right-handed; ROI, Region of interest; RSN, Resting-state network; S1, Primary somatosensory cortex; SD, Standard deviation; SMA, Supplementary motor area; STG, Superior temporal gyrus; SVV, Subjective visual vertical; TP, Temporo-parietal; U, Unique voxel; V1–5, Primary, secondary and tertiary visual cortices; VOG, Video-oculography; VOR, Vestibular-ocular reflex; VPS, Visual posterior sylvian area

* Corresponding author at: Department of Neurology, Ludwig-Maximilians Universität, Munich, Germany.

E-mail address: valerie.kirsch@med.lmu.de (V. Kirsch).

¹ These authors contributed equally.

<https://doi.org/10.1016/j.dib.2019.01.014>

2352-3409/© 2019 The Authors. Published by Elsevier Inc. This is an open access article under the CC BY-NC-ND license (<http://creativecommons.org/licenses/by-nc-nd/4.0/>).

component analysis (ICA). The data have been made publicly available via github (<https://github.com/RainerBoegle/BeyondBinaryParcellationData>).

© 2019 The Authors. Published by Elsevier Inc. This is an open access article under the CC BY-NC-ND license (<http://creativecommons.org/licenses/by-nc-nd/4.0/>).

Specifications table

Subject area	Neuroscience, Vestibular system
More specific subject area	Handedness-dependent organizational patterns of (lateralized and non-lateralized) functional subunits within the human vestibular cortical network
Type of data	Tables, figures, text file, data set
How data were acquired	3T Magnetic resonance imaging (MRI) data, 32-channel head coil, T2*-weighted echo-planar imaging (EPI) sequence, T1-weighted magnetization-prepared rapid gradient echo (MP-RAGE) sequence, task-free resting state.
Data format	Analyzed, Nifti *.nii files, MATLAB *.mat files, Portable Network Graphics *.png files, Text *.txt files
Experimental factors	30 healthy right-handed (RH) volunteers and 30 age- and gender-matched healthy left-handed (LH) volunteers with a verified sound vestibular system (semicircular and otolith function)
Experimental features	The multisensory (non-binary) nature of the human (vestibular) cortex was addressed by using binary and non-binary variations of independent component analysis (ICA) to separate its functional subunits.
Data source location	Munich, Germany, Latitude 48°06'22.20" N, Longitude 11°28'5.99" E
Data accessibility	The analyzed data are available within this article, the used dataset can be downloaded from the GitHub Link: https://github.com/RainerBoegle/BeyondBinaryParcellationData

Value of the data

- Proposition of a functional connectivity based parcellation (fCBP) approach that addresses the multisensory (non-binary) nature of the human vestibular cortex, here vestibular.
- Two variations of independent component analysis (ICA) are used: The traditional (binary) ICA approach, where each functional sub-unit must be spatially distinct (and voxels are forced to choose a sub-unit). And a variation, the multivariate (non-binary) ICA approach where functional-subunits can overlap (and voxels can be part of multiple sub-units with their various behavioral interpretations).
- This non-binary methodical approach might be able to reflect multiple signals at the same spatial location, e.g. in multiple populations of neurons or a single multisensory population.

1. Data

This data set aims to identify handedness-dependent organizational patterns of functional subunits within the human vestibular cortex whilst addressing its multisensory (non-binary) nature. To that end, 60 healthy volunteers (30 left-handed and 30 right-handed) were analyzed using a masked binary and non-binary fCBP (functional connectivity based parcellation) approach. This mask was

data-driven (composed of whole brain independent components) and specific to the vestibular cortical system as the used independent components (ICs) were required to include vestibular reference coordinates derived from two meta-analyses of vestibular neuroimaging experiments pinpointing the vestibular cortex [2,3].

2. Experimental design, materials and methods

Age- and gender-matched 30 left-handed (LH; 14 females; aged 20–65 years, mean age 26.1 ± 8.6 years) and 30 right-handed (RH; 17 females; aged 20–67 years, mean age 26.7 ± 8.3 years) healthy volunteers with a verified sound vestibular system (semicircular and otolith function) were examined on a 3T MR scanner (Magnetom Verio, Siemens Healthcare, Erlangen, Germany) using task free resting state functional MRI (fMRI) (Tables 1–3C).

After Preprocessing, the data were analyzed in four major steps using a functional connectivity based parcellation (fCBP) approach: (1) independent component analysis (ICA) on a whole brain level to identify different resting state networks (RSN); (2) creation of a vestibular informed mask from four whole brain ICs that included reference coordinates of the vestibular network extracted from meta-analyses of vestibular neuroimaging experiments; (3) Re-ICA confined to the vestibular informed mask; (4) cross-correlation of the activated voxels within the vestibular subunits (parcels) to each other (P-to-P) and to the whole-brain RSN (P-to-RSN). For a flowchart of the used functional connectivity based parcellation (fCBP) methods please view Fig. 1 of [1] (Figs. 1–4).

All details as well as further explanations of the methods can be viewed in the original publication, <https://doi.org/10.1016/j.neuroimage.2018.05.018> [1].

Table 1

Overview of used behavioral Interpretations of intrinsic whole brain resting-state networks (RSN).

Whole brain ICs	RSN	Name and anatomical allocation	Functional interpretation of networks
IC65, IC67	1	Limbic and medial-temporal areas BA 28/34/25/26/38, parahippocampal gyri	<ul style="list-style-type: none"> • Discrimination of emotional faces and pictures • Interoceptive processing
	2	Subgenual ACC and OFC BA 25/10-12	<ul style="list-style-type: none"> • Olfaction, gustation • Emotion
IC45, IC75	3	Bilateral basal ganglia and thalamus	<ul style="list-style-type: none"> • Wide range of mental processes (reward, non-painful thermal stimulation and interoceptive functions) • Relevant to motor, pain, and somatosensory processing
IC15, IC17	4	Bilateral anterior insula/frontal opercula & anterior aspect of the cingulate gyrus (BA13/16 and BA24)	<ul style="list-style-type: none"> • Transitional network linking cognition and emotion/interoception • Complex set of language, executive function, affective, and interoceptive processes, as well as auditory, pain, and gustatory processes
	5	Midbrain	<ul style="list-style-type: none"> • Sensorimotor functions and autonomic processes • Interoceptive stimulation
IC21, IC33, IC35, IC38, IC48	6	Superior and middle frontal gyri Premotor & supplementary motor cortices (SMA; BA 6) and FEFs (BA 8/9)	<ul style="list-style-type: none"> • Cognitive control of visuomotor timing • Preparation of movements
IC02, IC10, IC37, IC39	7	Middle frontal gyri and superior parietal lobules Dorsolateral prefrontal (BA 46) & posterior parietal cortices (BA 7)	<ul style="list-style-type: none"> • Visuospatial processing and reasoning • Adaptive control and stable maintenance functions
IC04, IC06, IC19, IC36, IC52	8	Ventral precentral gyri, central sulci, postcentral gyri, superior and inferior cerebellum Incl. primary sensorimotor cortices for upper extremities (M1; S1; BA 4/3/1/2)	<ul style="list-style-type: none"> • Action and somesthesia corresponding to hand movements
IC05, IC34, IC41	9	Superior parietal lobule Incl. medial posterior parietal association area (BA 5)	<ul style="list-style-type: none"> • Motor execution and learning
	10	Middle and inferior temporal gyri Incl. the middle temporal visual association area (MT,	<ul style="list-style-type: none"> • Viewing complex, often emotional stimuli • Mental rotation and the discrimination of locations in space.

Table 1 (continued)

		MST, V5; BA 37/39) at the temporo-occipital junction	
IC07, IC09, IC16	11	Lateral and medial posterior occipital cortices	<ul style="list-style-type: none"> • Simple visual stimuli & higher- level visual processing • Weak loadings across many fields, such as behavioral domain
IC08, IC11, IC27, IC44	12	primary, secondary, and tertiary visual cortices (V1, V2, V3; BA 17/18/19)	
IC14, IC22, IC26, IC53, IC59	13	Medial prefrontal and posterior cingulate/precuneus areas	<ul style="list-style-type: none"> • Default mode network • Theory of mind and social cognition tasks
IC51, IC57, IC62, IC70, IC74	14	Cerebellum	<ul style="list-style-type: none"> • Action and somesthesia • Range of sensorimotor, autonomic, and cognitive functions
IC12, IC25, IC28	15	Right-lateralized fronto-parietal regions	<ul style="list-style-type: none"> • Multiple cognitive processes
		Incl. right BA 44/45 and 22/39/40	
IC03, IC24	16	Transverse temporal gyri	<ul style="list-style-type: none"> • Audition (including tone and pitch discrimination), music and speech
		Incl. primary auditory cortices (A1; BA 41/42)	
IC01, IC40	17	Dorsal precentral gyri, central sulci, postcentral gyri, superior and inferior cerebellum	<ul style="list-style-type: none"> • Action and somesthesia corresponding to speech
		Incl. primary sensorimotor cortices for mouth (M1, S1; BA 4/ 3/1/2)	
IC18, IC23, IC55, IC60	18	Left-lateralized fronto-parietal regions	<ul style="list-style-type: none"> • Language • Memory, incl. working memory
		Incl. Broca's (BA 44/45) and Wernicke's (BA 22/39/40)	
	19	Artifacts*	<ul style="list-style-type: none"> • Template mismatch errors • Algorithmic abnormality occurring during spatial normalization
IC20	20		
IC13	21	Posterior and middle insula	<ul style="list-style-type: none"> • Emotional processing • Vestibular processing
IC21, IC29, IC42	22	Temporal pole, frontal orbital cortex and inferior frontal gyrus	<ul style="list-style-type: none"> • Semantic, word/language production & comprehension • Memory functions • Emotion, inhibition, theory of mind
IC30, IC63	23	Middle temporal gyrus, angular gyrus, supramarginal gyrus	<ul style="list-style-type: none"> • Face recognition, mentalizing • Audio-visual processing
IC32	24	Lateral occipital cortex	<ul style="list-style-type: none"> • Visual processing, observation, motion, eye movements
IC43, IC49, IC54, IC56, IC61, IC64, IC68, IC69, IC71-73, IC76-80	25	Frontal pole	<ul style="list-style-type: none"> • Executive functions, inhibition, • Memory functions • Social cognition • Mentalizing, default mode network
IC46	26	Middle frontal gyrus	<ul style="list-style-type: none"> • Decision making, autobiographical, self-referential
IC58	27	Rolandic operculum	<ul style="list-style-type: none"> • Emotional processing • Pain, somatosensory, social interaction

RSN1-20 was characterized as per Laird et al. [4]. Here, RSN 1-5 were accorded to “emotional and autonomic processes, perception”; RSN 6-9 to “mixture of functions related to motor and visuospatial integration, coordination, and execution”, RSN 10-12 to “Networks related to visual perception”, RSN10-18 to “divergent networks”. (*) RSN19-20 was defined as frequent artifacts. In addition, seven further RSN were defined using anatomical knowledge if they did not fit any of the Laird atlas RSN components. To assign a sound function to these 7 extra RSNs the maximum xyz-MNI-coordinates were entered in the Neurosynth platform (neurosynth.org) with a radius of 4 mm. The most plausible associations given by this automated synthesis with large-scale human functional neuroimaging data [5] were chosen and specified using main concept terms such as „emotional processing“. Each of the 27 RSNs was assigned to a separate color (cp. color scale), which matches the colors used for RSN-affiliations of whole brain IC maps in Fig. 2 of [1].

Abr.: A1 = primary auditory cortex; ACC = anterior cingulate cortex, BA = Broadman areal, FEF = frontal eye fields, IC = independent component; M1 = primary motor cortex; MST = medial superior temporal area; MT = middle temporal area; OFC = orbitofrontal cortex, RSN = resting-state network; S1 = primary somatosensory cortex; SMA = supplementary motor area, V1-5 = primary, secondary and tertiary visual cortices.

Table 2A
Characterization of “asymmetrical and less connected” parcels.

LH				RH				
Correlation to whole brain RSN	Anatomical location and cytoarchitectonic allocation	V	L-I	P +/-	V	L-I	Anatomical location and cytoarchitectonic allocation	Correlation to whole brain RSN
“IFG”								
4, 6, 22, 23, 25	55 % Inferior frontal gyrus R 11% Middle temporal gyrus R 54% Broca's area BA45 R/L 17% Broca's area BA44 R/L	309	1	2 +	-1	396	55% Inferior frontal gyrus L 11% Frontal operculum gyrus L 34 % Broca's area BA45 L 32 % Broca's area BA44 L	1, 6, 8, 10, 13, 14, 16, 18, 22, 23, 25
6, 8, 13, 14, 16, 18, 22, 23, 25	62% Inferior frontal gyrus L 43% Broca's area BA44 L 23% Broca's area BA45 L	371	-95	21 +	97	198	79% Inferior frontal gyrus R 58% Broca's area BA44 R 38% Broca's area BA45 R	1, 4, 6, 10, 15, 17, 18, 22, 23, 25
“S/MTG”								
6, 12, 16, 22, 23	35% Superior temporal gyrus R 30% Middle temporal gyrus R 13% Supramarginal gyrus R50% N/A 15% Inferior parietal lobule PF R 5% Insula Id1 R	578	66	4 -	76	650	30% Middle temporal gyrus R 25% Superior temporal gyrus R 21% Supramarginal gyrus R 50% N/A 27% Inferior parietal lobule PF, Pfm, Pga R 2% Insula Id1 R	3, 7, 10, 11, 12, 15, 16, 22, 23, 24, 25
“Middle and posterior insula”								
21	46% Planum polare R 20% Superior temporal gyrus R 40% N/A 22% GM Insula Id1 R 5% Inferior parietal lobule PF R	92	93	5 +	-88	103	42% Insular cortex L 28% Temporal pole L 19% Frontal orbital cortex L 95% N/A	4, 7, 12, 14, 20, 21, 27
21	31% Temporal pole L 28% Planum polare L 52% N/A 8% Insula Id1 L 6% Inferior parietal lobule PF L 6% Hippocampus entorhinal cortex R	97	-51	13 +	46	217	34% Planum polare R 26% Insular cortex R 27% Insula Id1 R 12% N/A 8% Insula Id1 L 8% Primary auditory cortex TE1.0 R	8, 13, 14, 15, 16, 18, 21, 23, 25,
4, 6, 7, 8, 9, 15, 16, 18, 21, 22, 23, 25	19% Temporal pole R 16% Parietal operculum cortex R 12% Supramarginal gyrus R 30% Inferior parietal lobule PF, PfcM, PFop L	217	24	17 +	-57	216	17% Planum temporale L 23% Insular cortex L/R 13% Superior temporal gyrus L 26% Inferior parietal lobule PF, PfcM L	3, 4, 6, 8, 9, 14, 16, 18, 23, 25, 27
	21% N/A 5% Insula Id1 R						18% Insula Id1 L/R 17% N/A	
12, 13, 18, 21	54% Insular cortex L/R 22% Planum polare L 15% Temporal pole L 39% N/A 17% Insula Id1 L/R 12% Primary auditory cortex TE1.2 L	211	-62	25 +	42	159	30% Temporal pole R 28% Inferior frontal gyrus R 17% Insular cortex L 45% N/A 28% Broca's area BA45 R 10% Insula Id1 L	13, 14, 17, 18, 21, 23, 25
3, 4, 6, 8, 12, 15, 16, 18, 21, 23, 27	18% Insular cortex L/R 18% Heschl's gyrus L/R 16% Planum temporale L/R 8% Supramarginal gyrus L 19% N/A 12% Insula Id1 L/R + Ig2 R 16% Primary auditory cortex TE1.0 L + TE 1.1 L/R 8% Inferior parietal lobule PfcM L	668	-40	28 +	12	514	15% Precentral gyrus L 15% Central opercular cortex R 11% Middle temporal gyrus R 8% Insular cortex L 42% N/A 12% Secondary somatosensory cortex OP4, 3 R 5% Secondary somatosensory cortex OP1 L 6% Broca's area BA44 L 5% Premotor cortex BA6 L	3, 16, 17, 18, 25, 27
6	20% Supramarginal gyrus L 17% Central opercular cortex L 11% Middle temporal gyrus R 8% Superior temporal gyrus R 45% N/A 18% Inferior parietal lobule PF + Pfm L 17% Secondary somatosensory cortex OP4 L	186	-18	30 -	-8	375	18% Central opercular cortex L 13% Temporal pole R 11% Supramarginal gyrus L 8% Superior temporal gyrus R 41% N/A 17% Secondary somatosensory cortex OP4 L 10% Inferior parietal lobule Pfm + PF L 4% Insula Id1 R	12, 16, 17, 23
“Inferior insula”								
21, 25	80% Temporal pole R 4% Frontal orbital cortex R 87% N/A 3% Amygdala laterobasal group L/R	45	93	18 +	-100	43	81% Temporal pole L 19% Frontal orbital cortex L 93% N/A 3% Amygdala laterobasal group L	1, 21
1, 3, 7, 11, 12, 15, 21	82% Temporal pole L 7% Insular cortex L 4% Planum polare L 95% N/A	87	-96	19 +	92	49	67% Temporal pole R 14% Insular cortex R 6% Parahippocampal gyrus R 71% N/A 8% Hippocampus entorhinal cortex R	1, 4, 12, 13, 14, 15, 21, 25
1, 3, 6, 17	30% Temporal pole R 21% Parahippocampal gyrus R			23			44% Temporal pole R 32% Parahippocampal gyrus R	15, 21, 25

Table 2A (continued)

	16% Inferior frontal gyrus R 15% Frontal orbital cortex R 27% N/A 24% Hippocampus entorhinal cortex R 22% Amygdala laterobasal and superficial group R 17% Broca's area BA44 + BA45 R 4% Insula Id1 R	179	89	-	100	97	22% Frontal orbital cortex R 41% Hippocampus entorhinal cortex R 36% N/A 20% Amygdala laterobasal and superficial group R 2% Insula Id1 R	
18, 21	63% Temporal pole R 18% Superior temporal gyrus R 16% Insular cortex R 89% N/A 2% Hippocampus entorhinal cortex R	57	100	24 +	-92	75	59% Temporal pole L 28% Planum polare 61% N/A 9% Insula Id1 L 5% Hippocampus entorhinal cortex L	1, 4, 21
1, 3, 8	71% Temporal pole L 14% Frontal orbital cortex L 6% Superior temporal gyrus L 2% Insular cortex L 83% N/A	70	-86	26 +	79	38	34% Temporal pole R 24% Frontal orbital cortex R 11% Insular cortex R 8% Superior temporal gyrus R 97% N/A	13, 21, 23, 25
21	81% Temporal pole R 14% Frontal orbital cortex R 97% N/A 2% Hippocampus entorhinal cortex R	43	91	27 +	-91	65	66% Temporal pole L 14% Frontal orbital cortex L 58% N/A 32% Amygdala laterobasal + superficial group L 12% Hippocampus entorhinal cortex L	1, 10, 18, 21
1, 10, 13, 14, 25, 27	38% Temporal pole L/R 12% Postcentral gyrus R 11% Frontal orbital cortex L 43% N/A 19% Amygdala laterobasal + superficial group L 15% Hippocampus entorhinal cortex L 4% Primary somatosensory cortex BA1 R	169	-31	29 +	40	43	63% Temporal pole R 23% Planum polare L 5% Insular cortex L 47% N/A 21% Insula Id1 L/R 14% Amygdala laterobasal group R	3, 4, 6, 7, 8, 17, 18, 21, 25

Masked Binary and non-binary fCBP (functional connectivity brain parcellation) resulted in 30 different parcels, which were categorized by means of “spatial symmetry”, “number of parcels to systems correlations” and “predominant anatomical landmark”. This resulted in two different types of parcels: “Asymmetrical and less connected” (Table 2A) and “symmetrical and connected” (Table 2B) voxels (V). Each of the 30 parcels (P) was assigned to a separate color (cp. color scale Fig. 3 of [1]), which was the same in both LH (left-handed) and (RH) right-handed subgroups. “Asymmetrical” parcels were highlighted in grey. Parcels were anatomically characterized using the Harvard- Oxford structural cortical atlas in bold letters [6,7] and the Jülich histological (cyto- and myeloarchitectonic) atlas in regular letters [8,9]. Handedness-dependency (+/-) was calculated using a laterality index. If the laterality-index (L-I) per parcel and in between LH and RH changed concordant it was termed handedness-independent (-). An inverse laterality-index was termed handedness-dependent (+).

Table 2B

Characterization of “symmetrical & connected” parcels.

Correlation to whole brain RSN	LH					RH				
	Anatomical location and cytoarchitectonic allocation	V	L-I	P +/-	L-I	V	Anatomical location and cytoarchitectonic allocation	Correlation to whole brain RSN		
“Anterior insula”										
3, 4, 6, 9, 10, 13, 15, 16, 18, 21, 22, 25	47% Insular cortex L/R 41% Frontal orbital cortex L/R 10% Temporal pole L/R 80% N/A 5% Broca's area BA44 and BA45 R	163	-4	6 +	76	295	31% Frontal orbital cortex R/L 25% Insular cortex R/L 19% Frontal operculum Cortex L/R 12% Temporal pole R 58% N/A 25% Broca's area BA44 and BA45 R	1, 4, 6, 7, 8, 10, 11, 12, 13, 15, 16, 17, 21, 22, 24, 25, 26		
3, 4, 6, 7, 8, 10, 11, 12, 13, 14, 15, 16, 17, 18, 21, 22, 23, 24, 25	50% Insular cortex R/L 21% Frontal operculum cortex L/R 8% Frontal orbital cortex R 52% N/A 29% Broca's area BA44 L/R and BA 45L/R	401	29	14 +	-8	285	70% Insular cortex L/R 7% Frontal operculum cortex L 6% Central opercular cortex L 48% N/A 25% Broca's area BA44 L/R	1, 3, 4, 6, 7, 10, 15, 16, 18, 22, 23, 25, 27		
“Sensorimotor”										
1, 3, 4, 6, 7, 8, 9, 11, 12, 13, 14, 15, 16, 17, 18, 21, 22, 24, 25, 20, 27	51% Postcentral gyrus L/R 33% Precentral gyrus L/R 22% Secondary somatosensory cortex OP4 L/R 32% Primary somatosensory cortex BA3a+b R/L 9% Primary somatosensory cortex BA1 L/R 5% Primary motor cortex BA4p L/R 5% Premotor cortex BA6 L/R	888	1	1 +	-1	780	57% Postcentral gyrus L/R 30% Precentral gyrus L/R 22% Secondary somatosensory cortex OP4 L/R 30% Primary somatosensory cortex BA3a+b L/R 10% Primary somatosensory cortex BA1 L/R 6% Premotor cortex BA6 L/R 5% Primary motor cortex BA4p L/R	1, 6, 7, 8, 9, 11, 12, 14, 16, 17, 21, 22, 24, 27		
3, 4, 6, 8, 9, 12, 14, 15, 16, 17, 18, 22, 24, 27	51% Precentral gyrus L/R 46% Postcentral gyrus L/R 27% Primary somatosensory cortex BA1 L/R 23% Premotor cortex BA6 R/L 17% Primary motor cortex BA4p +a L/R 8% Primary somatosensory cortex BA3a+b L/R	353	-10	3 -	-10	532	51% Precentral gyrus L/R 37% Postcentral gyrus L/R 22% Primary somatosensory cortex BA1 L/R 14% Premotor cortex BA6 L/R 24% Primary somatosensory cortex BA3a+b L/R 15% Primary somatosensory cortex BA3b L/R	3, 4, 6, 7, 8, 9, 11, 12, 14, 15, 16, 17, 21, 22, 24, 25		
“STG”										
1, 4, 6, 7, 8, 13, 14, 15, 16, 18, 21, 22, 23, 25	32% Temporal pole R 14% Central opercular cortex R 13% Inferior frontal gyrus R	153	95	10 +	-87	251	47% Temporal pole L/R 15% Superior temporal gyrus L 14% Planum polare L/R	4, 6, 7, 9, 10, 11, 12, 15, 16, 18, 21, 22, 23, 25		

Table 2B (continued)

	13% Insular cortex R 4% Frontal orbital cortex R 39% N/A 32% Broca's area BA44 R 7% Secondary somatosensory cortex OP4 R 6% Inferior parietal lobule PF R						6% Frontal orbital cortex L 4% Insular cortex L 63% N/A 14% Primary auditory cortex TE1.2 L 14% Broca's area BA44 L + BA45 L			
3, 4, 6, 7, 8, 9, 10, 11, 12, 14, 15, 16, 17, 18, 21, 22, 23, 24, 25, 27	46% Superior temporal gyrus L/R 23% Planum temporale L 8% Middle temporal gyrus R 46% N/A 35% Secondary somatosensory cortex OP1/4 L 10% Inferior parietal lobule PF L 5% Primary auditory cortex TE1.0 L	112	-39	-	12	-58	530	30% Superior temporal gyrus L 20% Middle temporal gyrus L/R 30% Temporal pole R/L 65% N/A 9% Secondary somatosensory cortex OP1 L 7% Primary auditory cortex TE1.0 L 7% Inferior parietal lobule PF L	3, 4, 6, 7, 8, 9, 10, 11, 12, 13, 14, 15, 16, 18, 20, 23, 24, 25	
1, 4, 6, 7, 8, 9, 10, 11, 12, 16, 17, 18, 20, 22, 25, 27	33% Superior temporal gyrus R 21% Planum polare R 12% Central opercular cortex R 7% Temporal pole R 35% N/A 32% Primary auditory cortex TE 1.0 R + TE1.2 R 11% Secondary somatosensory cortex OP4 R	201	85	-	15	93	173	42% Superior temporal gyrus R 25% Temporal pole R 6% Planum temporale R 75% N/A 13% Primary auditory cortex TE1.2 R 5% Primary auditory cortex TE1.0 R	1, 6, 7, 9, 11, 12, 13, 14, 16, 17, 20, 22, 23, 24, 25, 26	
3, 4, 6, 7, 8, 9, 10, 11, 12, 13, 14, 15, 16, 17, 18, 20, 22, 23, 24, 25	40% Postcentral gyrus L/R 18% Middle temporal gyrus R 8% Parietal operculum cortex L 8% Temporal pole R 41% N/A 16% Secondary somatosensory cortex OP1 L 12% Inferior parietal lobule PFT L 8% Primary somatosensory cortex BA1 + BA2 L	446	-26	+	16	66	216	52% Superior temporal gyrus R/L 25% Planum temporale R/L 8% Temporal pole R 56% N/A 20% Primary auditory cortex TE1.0+1.1+1.2 R 11% Inferior parietal lobule PF R	7, 8, 9, 11, 14, 22, 23, 25	
1, 3, 6, 7, 8, 9, 10, 11, 12, 14, 16, 17, 22, 23, 24, 25, 27	35% Superior temporal gyrus L 12% Middle temporal gyrus L 9% Planum temporale L 6% Central opercular cortex L 6% Heschl's gyrus L 45% N/A 23% Primary auditory cortex TE1.2 +1.0 L 12% Secondary somatosensory cortex OP4 L	371	-85	-	20	-98	131	52% Superior temporal gyrus L 11% Central opercular cortex L 10% Planum polare L 8% Precentral gyrus L 41% N/A 23% Secondary somatosensory cortex OP4 L 18% Primary auditory cortex TE1.2 L 8% Broca's area BA44 L	3, 4, 6, 8, 9, 14, 15, 16, 17, 18, 21, 22, 25, 27	
	3% Primary somatosensory cortex BA1 L							5% Primary somatosensory cortex BA1 L		
1, 3, 6, 7, 8, 9, 10, 11, 12, 16, 17, 20, 22, 24, 27	59% Temporal pole R 12% Central opercular cortex R 7% Postcentral gyrus R 5% Superior temporal gyrus R 71% N/A 19% Secondary somatosensory cortex OP4 R	150	100	-	22	84	131	34% Central opercular cortex R 15% Planum temporale R 15% Superior temporal gyrus R 14% Postcentral gyrus R 31% N/A 31% Secondary somatosensory cortex OP4 R 20% Secondary somatosensory cortex OP1 R	1, 6, 7, 8, 9, 10, 11, 16, 17, 21, 22, 24, 27	
"Temporo-parietal"										
1, 3, 6, 7, 8, 9, 10, 11, 12, 14, 16, 17, 18, 20, 22, 24, 27	20% Central opercular cortex R 19% Planum temporale R 15% Heschl's gyrus R 10% Superior temporal gyrus R 37% Primary auditory cortex TE1.0 + TE1.1 R/L 29% Secondary somatosensory cortex OP1 R/L 8% Secondary somatosensory cortex OP4 R	309	48	-	7	25	503	32% Parietal operculum cortex L/R 26% Planum temporale L/R 6% Central opercular cortex R 32% Secondary somatosensory cortex OP1 R/L 20% Inferior parietal lobule PFcm R/L 16% Primary auditory cortex TE1.0 + TE1.1 R/L 11% Inferior parietal lobule PF R + PfoP L	1, 4, 6, 7, 8, 9, 12, 13, 15, 16, 17, 22, 27	
3, 6, 8, 11, 12, 17, 22, 25, 27	39% Precentral gyrus R 11% Inferior frontal gyrus R 10% Supramarginal gyrus R 8% Insular cortex R 30% Broca's area BA44 R 14% Premotor cortex BA6 R 12% Secondary somatosensory cortex OP3 R 15% Inferior parietal lobule PFT, PF, PFCm R	411	84	-	8	35	547	45% Postcentral gyrus L/R 24% Supramarginal gyrus R 15% Precentral gyrus R 4% Insular cortex R 43% Inferior parietal lobule PfoP + PFT L/R 9% Broca's area BA44 R 9% Secondary somatosensory cortex OP1+3 R 4% Premotor cortex BA6 R	1, 6, 7, 8, 9, 10, 11, 12, 13, 14, 16, 17, 18, 22, 24, 25, 27	
1, 4, 6, 7, 8, 9, 11, 12, 13, 16, 17, 18, 22, 23, 25, 27	20% Precentral gyrus L 23% Temporal pole L/R 17% Central opercular cortex L 37% Broca's area BA44 L/R 20% Secondary somatosensory cortex OP4 L/R 5% Primary auditory cortex TE1.2 L/R	139	-51	+	9	94	140	23% Precentral gyrus R 17% Central opercular cortex R 16% Inferior frontal gyrus R 43% Broca's area BA44 R 15% Secondary somatosensory cortex OP4 R 11% GM Primary auditory cortex TE1.2 R 9% Inferior parietal lobule PF R	1, 4, 6, 7, 8, 9, 10, 13, 14, 15, 16, 17, 18, 20, 21, 22, 24, 25, 27	
1, 4, 6, 8, 9, 13, 14, 15, 16, 17, 18, 22, 25, 27	28% Precentral gyrus L 16% Insular cortex L 12% Central opercular cortex L 26% Broca's area BA44 L 12% Inferior parietal lobule PfoP, PF, PFT L 6% Premotor cortex BA6 L 6% Secondary somatosensory cortex OP4 L	518	-66	-	11	-57	377	64% Precentral gyrus L/R 19% Inferior frontal gyrus L 8% Central opercular cortex L	1, 4, 6, 8, 10, 12, 13, 15, 17, 18, 22, 24, 25, 27	

Masked Binary and non-binary fCBP (functional connectivity brain parcellation) resulted in 30 different parcels, which were categorized by means of "spatial symmetry", "number of parcels to systems correlations" and "predominant anatomical landmark". This resulted in two different types of parcels: "Asymmetrical and less connected" (Table 2A) and "symmetrical and connected" (Table 2B) voxels (V). Each of the 30 parcels (P) was assigned to a separate color (cp. color scale Fig. 3 of [1]), which was the same in both LH (left-handed) and (RH) right-handed subgroups. "Asymmetrical" parcels were highlighted in grey. Parcels were anatomically characterized using the Harvard-Oxford structural cortical atlas in bold letters [6,7] and the Jülich histological (cyto- and myeloarchitectonic) atlas in regular letters [8,9]. Handedness-dependency (+/-) was calculated using a laterality index. If the laterality-index (L-I) per parcel and in between LH and RH changed concordant it was termed handedness-independent (-). An inverse laterality-index was termed handedness-dependent (+).

Table 3A

Characterization of "unique voxels" within parcels, type "asymmetric and less connected".

LH			RH			
Anatomical location and cytoarchitectonic allocation	V	L-I	U +/-	L-I	V	Anatomical location and cytoarchitectonic allocation
"IFG"						
68 % Inferior frontal gyrus R 15% Middle temporal gyrus R 8% Angular Gyrus R 62% Broca's area BA45 R 23% Inferior parietal lobule PFm, Pga R	72	100	U2 +	-100	129	75% Inferior frontal gyrus L 19% Frontal operculum gyrus 54 % Broca's area BA45 L 38 % Broca's area BA44 L
56% Inferior frontal gyrus L 15% Middle temporal gyrus L 6% Frontal orbital cortex L 5% Superior temporal gyrus L 41% N/A 34% Broca's area BA44 L 22% Broca's area BA45 L	149	-100	U21 +	100	95	88% Inferior frontal gyrus R 6% Frontal operculum Cortex R 48% Broca's area BA44 R 48% Broca's area BA45 R
"S/MTG"						
49% Superior temporal gyrus R 19% Supramarginal gyrus R 8% Middle temporal gyrus R 52% N/A 13% Inferior parietal lobule PF R 11% Insula Id1 R	191	80	U 4 -	100	244	31% Superior temporal gyrus R 28% Supramarginal gyrus R 28% Middle temporal gyrus R 52% N/A 36% Inferior parietal lobule PF, PFm, Pga R 5% Insula Id1 R
"Middle and posterior insula"						
			U5	-100	16	69% Insular cortex L 25% Frontal orbital cortex L 6 % Temporal pole L 87% N/A
			U13			
41% Planum polare R 29% Insular Cortex R 29% N/A 18% Insula Id1 R 6 % Hippocampus cornu ammonis R	17	100	U17 +	-40	60	20% Insular cortex L 20% Planum polare L 18% N/A 5% Superior temporal gyrus L 48% Insula Id1 L/R 5% Amygdala centromedian group L
			U25	100	16	94% Inferior frontal gyrus R 6% Frontal pole R 87% Broca's area BA45 R 12% N/A

Table 3A (continued)

			U24			
			U26			
87% Temporal pole R 13% Frontal orbital cortex R 100% N/A	15	100	U27 +	-100	16	50% Temporal pole L 44% Frontal orbital cortex L 6% Parahippocampal gyrus L 68% N/A 19% Hippocampus entorhinal cortex L 6% Amygdala laterobasal group L
47% Temporal pole L 26% Parahippocampal gyrus L 24% Frontal orbital cortex L 37% N/A 36% Hippocampus entorhinal cortex L 21% Amygdala laterobasal + superficial group L	53	-100	U29			
26% Insular cortex L/R 12% Heschl's gyrus L/R 10% Planum polare L/R 10% Supramarginal gyrus L 7% Superior temporal gyrus L 5% N/A 25% Insula Id1 L/R + Ig2 L/R 19% N/A 8% Inferior parietal lobule PFcm L	323	-45	U28 +	45	184	18% Middle temporal gyrus R 24% Central opercular cortex R/L 23% Temporal pole R/L 11% N/A 5% Insular cortex R 43% N/A 8% Secondary somatosensory cortex OP4 R 5% Secondary somatosensory cortex OP3 R 8% Secondary somatosensory cortex OP1 L 8% Amygdala superficial group R
			U30	-11	83	27% Central opercular cortex L 10% Planum polare L 10% Angular gyrus L 10% Precentral gyrus R 8% Supramarginal gyrus L 7% Insular cortex L 5% Middle temporal gyrus R 5% Superior temporal gyrus R 27% N/A 27% Secondary somatosensory cortex OP4 L 5% Amygdala laterobasal group R 4% Insula Id1 R
"Inferior insula"						
			U18			
			U19			
30% Temporal pole R 30% Frontal orbital cortex R 30% Parahippocampal gyrus R 44% Amygdala laterobasal R 30% Hippocampus entorhinal cortex R	27	100	U23 -	100	32	56% Parahippocampal gyrus R 25% Temporal pole R 19% Frontal orbital cortex R 65% Hippocampus entorhinal cortex R 25% Amygdala laterobasal group R

Masked non-binary fCBP (functional connectivity based parcellation) enabled the distinction of spatial uniqueness (Tables 3A and 3B) and commonality (3C) of independent components that form parcels. Analog to Tables 2A and 2B "unique voxels" (U) were left in the previous categorization in two types of "unique" voxels: Type previously "asymmetric and less connected" (Table 3A, highlighted in grey) and type previously "symmetric and connected" (Table 3B). An inverse laterality-index (L-I) was termed handedness-dependent (+), a concordant laterality-index meant handedness-independency (-). Common" voxels were defined as voxels that overlapped in between parcels. To enable visualization of the "common" voxels, 9 groups of 2-6 spatially similar parcels ("common clusters"; C) were defined and correlated to whole brain RSN.

For a depiction of "unique" voxels please view Fig. 6A in [1], and for the "common clusters" view Fig. 6B in [1]. Each of the 30 parcels (P) was assigned to a separate color (cp. color scale Fig. 3 in [1]), which was also used for the parcel's "unique voxels". The colors match between (left-handed) LH and right-handed (RH) subgroups. This color-code can also be seen in Table 3C, where each color represents one of the parcels included in the "common" cluster. U and C were anatomically characterized using the Harvard-Oxford structural cortical atlas in bold letters [6,7] and the jülich histological (cyto- and myelo-architectonic) atlas in regular letters [8,9].

Table 3B

Characterization of “unique voxels” within parcels, type “symmetric and connected”.

LH			RH			
Anatomical location and cytoarchitectonic allocation	V	L-I	U +/-	L-I	V	Anatomical location and cytoarchitectonic allocation
“Anterior insula”						
			U6	100	76	54% Frontal orbital cortex R 31% Insular cortex R/L 9% Inferior frontal gyrus R 56% N/A 17% Broca's area BA45 R
28% Insular cortex R 21% Frontal operculum cortex R 11% Frontal orbital cortex R 32% N/A 17% Amygdala superficial group R 18% Broca's area BA44 and BA 45 R	54	100	U 14 +	-69	108	66% Insular cortex L/R 17% Central operculum cortex L 17% 21% Frontal operculum cortex L/R 43% Broca's area BA44 L/R 34% N/A
“Sensorimotor”						
55% Postcentral gyrus L/R 26% Precentral gyrus L/R 28% Secondary somatosensory cortex OP4 L/R 40% Primary somatosensory cortex BA3a+b R/L	276	10	U1 +	-11	147	61% Postcentral gyrus L/R 22% Precentral gyrus L/R 17% Central operculum cortex L/R 28% Secondary somatosensory cortex OP4 L/R 35% Primary somatosensory cortex BA3a+b L/R
58% Precentral gyrus L/R 41% Postcentral gyrus L/R 26% Primary somatosensory cortex BA1 L/R 16% Premotor cortex BA6 R/L 15% Primary somatosensory cortex BA3a+b L/R 28% Primary motor cortex BA4p L/R +a L	141	10	U3 +	-11	207	53% Postcentral gyrus L/R 45% Precentral gyrus L/R 28% Primary somatosensory cortex BA3a+b L/R 20% Primary motor cortex BA4a+p L 14% Premotor cortex BA6 L/R 10% Primary somatosensory cortex BA1 L
“STG”						
			U10	-100	34	64% Temporal pole L 24% Superior temporal gyrus L 8% Planum polare L/R 62% N/A 23% Primary auditory cortex TE1.2 L
			U12	-36	205	20% Superior temporal gyrus L 28% Temporal pole R/L 13% Middle temporal gyrus L/R
						80% N/A 4% Inferior parietal lobule PF L 2% Primary auditory cortex TE1.0 L
			U15	100	18	50% Superior temporal gyrus R 44% N/A 6% Precentral gyrus 95% N/A 6% Primary auditory cortex TE1.2 R
36% Middle temporal gyrus R 27% Postcentral gyrus L 13% Temporal pole R 7% Central opercular cortex L 7% Parietal operculum cortex L 65% N/A 14% Secondary somatosensory cortex OP1 L	189	2	U16 -	100	33	55% Superior temporal gyrus R 42% Planum temporale R 3% Heschl's Gyrus 58% N/A 33% Primary auditory cortex TE1.0+ 1.1 R
			U20	-100	27	78% Superior temporal gyrus L 11% Planum polare L 7% Central opercular cortex L 48% N/A 22% Primary auditory cortex TE1.2 L 22% Secondary somatosensory cortex OP4 L

Table 3B (continued)

			U22	100	35	37% N/A 29% Postcentral gyrus R 23% Superior temporal gyrus R 9% Central opercular cortex R 63% N/A 29% Secondary somatosensory cortex OP4 R 9% Secondary somatosensory cortex OP1 R	
"Temporo-parietal"							
33% Central opercular cortex R 22% Superior temporal gyrus R 17% Planum temporale R 11% Parietal operculum cortex R 11% Postcentral gyrus R 75% Secondary somatosensory cortex OP1 R 20% N/A	36	100	7	-	15	192	56% Parietal operculum cortex L/R 20% Planum temporale L/R 25% Insular cortex R 7% Central opercular cortex R 39% Secondary somatosensory cortex OP1 R/L 25% Inferior parietal lobule PFCm R/L 13% Primary auditory cortex TE1.0 +TE1.1 R/L
51% Precentral gyrus R 14% Central opercular cortex R 13% Insular cortex R 13% Supramarginal gyrus R 30% Broca's area BA44 R 22% Secondary somatosensory cortex OP3 R 14% Premotor cortex BA6 R	176	100	8	-	54	132	63% Postcentral gyrus L/R 28% Supramarginal gyrus R 65% Inferior parietal lobule PFop + PFT L/R 10% Secondary somatosensory cortex OP1+3 R
			9		100	30	37% Precentral gyrus R 27% Inferior frontal gyrus R 13% Temporal pole 7% Central opercular cortex R 73% Broca's area BA44 R 23% N/A
27% Precentral gyrus L 24% Insular cortex L 19% Central opercular cortex L 6% Supramarginal gyrus L 25% N/A 24% Broca's area BA44 L 9% Secondary somatosensory cortex OP4 L	220	-83	11	-	-67	118	70% Precentral gyrus L/R 17% Central opercular cortex L 11% Inferior frontal gyrus L 53% Broca's area BA44 L/R 6% Secondary somatosensory cortex OP4 L

Masked non-binary fCBP (functional connectivity based parcellation) enabled the distinction of spatial uniqueness (Tables 3A and 3B) and commonality (Table 3C) of independent components that form parcels. Analog to Tables 2A and 2B "unique voxels" (U) were left in the previous categorization in two types of "unique" voxels: Type previously "asymmetric and less connected" (Table 3A, highlighted in grey) and type previously "symmetric and connected" (Table 3B). An inverse laterality-index (L-I) was termed handedness-dependent (+), a concordant laterality-index meant handedness-independency (-). Common" voxels were defined as voxels that overlapped in between parcels. To enable visualization of the "common" voxels, 9 groups of 2-6 spatially similar parcels ("common clusters"; C) were defined and correlated to whole brain RSN.

For a depiction of "unique" voxels please view Fig. 6A in [1], and for the "common clusters" view Fig. 6B in [1]. Each of the 30 parcels (P) was assigned to a separate color (cp. color scale Fig. 3 in [1]), which was also used for the parcel's "unique voxels". The colors match between (left-handed) LH and right-handed (RH) subgroups. This color-code can also be seen in Table 3C, where each color represents one of the parcels included in the "common" cluster. U and C were anatomically characterized using the Harvard- Oxford structural cortical atlas in bold letters [6,7] and the Jülich histological (cyto- and myelo-architectonic) atlas in regular letters [8,9].

Table 3C
Characterization of “common” clusters (C).

LH			RH			
Correlation to whole brain RSN	Anatomical location and cytoarchitectonic allocation	V	Common Cluster	V	Anatomical location and cytoarchitectonic allocation	Correlation to whole brain RSN
7, 13, 16, 21, 27	48% Insular cortex L/R 53% Planum polare R/L 40% N/A 20% Insula Id1 L	298	C1 “Posterior insula” 	133	75% Insular cortex L/R 17% Temporale pole R 60% N/A 20% Insula Id1 L/R	1, 21
1, 21	48% Insular cortex L>R 33% Planum polare L>R 85% N/A 3% Hippocampus entorhinal cortex R	200	C2 “Inferior insula” 	219	81% Temporal pole L>R 80% N/A 5% Hippocampus entorhinal cortex L	1, 4, 15, 18, 21
4, 6, 17, 21, 22, 23, 25, 27	62% Frontal orbital cortex L/R 26% Inferior frontal gyrus L/R 60% N/A 25% Broca's area BA44 L/R 23% Broca's area 45 L/R 13% Temporal Pole L/R	269	C3 “IFG” 	282	25% Inferior frontal gyrus L 37% Planum polare L 25% Temporal pole L/R 12% Frontal orbital cortex R 62% N/A 25% Primary auditory cortex TE1.2 L 13% Broca's area BA44 L	4, 6, 7, 8, 9, 14, 15, 16, 18, 21, 22, 23, 25, 27
3, 6, 7, 8, 9, 11, 12, 14, 15, 16, 17, 18, 22, 24, 27	61% Precentral gyrus L/R 39% Postcentral gyrus L/R 42% Primary somatosensory cortex L/R BA1, BA31+b 20% Primary motor cortex BA4p L/R 19% Premotor cortex BA 6 L/R	147	C4 “Sensorimotor” 	235	64% Postcentral gyrus L/R 36% Precentral gyrus L/R 67% Primary somatosensory cortex L/R BA1, BA3a+b 14% Primary motor cortex BA4p L/R 7% Premotor cortex BA 6 L/R	3, 6, 8, 9, 11, 12, 14, 15, 16, 17, 27
1, 6, 7, 8, 9, 11, 12, 14, 16, 17, 21, 22, 23, 24, 27	37% Superior temporal gyrus L/R 13% Temporal pole R 12% Central opercular cortex R 7% Planum temporale R 53% N/A 25% Sec. somatosensory cortex OP4 L/R 21% Primary auditory cortex TE1.2 L/R	216	C5 “STG” 	76	44% Superior temporal gyrus L/R 27% Planum temporale L/R 9% Central opercular cortex R 8% Planum polare R 45% N/A 32% Sec. somatosensory cortex OP4 L/R 17% Primary auditory cortex TE1.2 R#	1, 6, 7, 8, 9, 14, 16, 27, 20, 21, 22, 23, 27
6, 12, 16, 17, 18, 22, 23, 27	63% Superior temporal gyrus L/R 27% Planum temporale L 5% Middle temporal gyrus R 47% N/A 27% Sec. somatosensory cortex OP1 L 11% Primary auditory cortex TE1.0 L 6% Inferior parietal lobule PF L	126	C6 “S/MTG” 	186	43% Superior temporal gyrus L/R 35% Middle temporal gyrus L/R 17% Supramarginal gyrus L 70% N/A 8% Inferior parietal lobule PFM L 8% Inferior parietal lobule PF L	4, 8, 11, 12, 13, 15, 16, 22, 23, 24, 27
3, 4, 6, 7, 8, 11, 13, 15, 18, 21, 22, 24, 25	65% Insular cortex L/R 24% Frontal orbital cortex L/R 7% Frontal opercular cortex R 68% N/A 11% Broca's area BA44+45 L/R	249	C7 “Anterior insula” 	123	60% Insular cortex L/R 25% Frontal opercular cortex R 7% Temporal pole R 56% N/A 25% Broca's area BA44+45 L/R	3, 4, 6, 7, 8, 10, 12, 13, 15, 16, 18, 21, 22, 24, 27
4, 6, 7, 8, 9, 11, 12, 14, 15, 16, 17, 18, 21, 22, 23, 24, 27	28% Planum temporale L/R 21% Heschl's gyrus L/R 9% Central opercular cortex L/R 8% Parietal operculum cortex L 8% Supramarginal gyrus L 21% Primary auditory cortex TE1.0 L/R 19% Inferior parietal lobule PF, PFCm, PFM L 12% Sec. somatosensory cortex OP1 L/R	614	C8 “Heschl Gyrus” 	915	15% Central opercular cortex L/R 11% Insular cortex L/R 11% Planum temporale L 11% Heschl's gyrus L/R 18% N/A 16% Primary auditory cortex TE1.0 L/R 14% Sec. somatosensory cortex L/R OP4 9% Sec. somatosensory cortex L/R OP1	4, 6, 7, 8, 9, 11, 12, 15, 16, 17, 18, 21, 22, 23, 24, 27
4, 6, 8, 13, 14, 16, 17, 18, 21, 22, 25, 27	35% Precentral gyrus L/R 17% Central opercular cortex L/R 15% Inferior frontal gyrus L/R 4% Postcentral gyrus L 53% Broca's area BA44 L/R 12% Sec. somatosensory cortex OP4 L/R 9% Primary auditory cortex TE1.2 L/R	337	C9 “temporo-parietal intersection” 	235	47% Precentral gyrus L/R 24% Supramarginal gyrus L/R 10% Postcentral gyrus L 32% Broca's area BA44 L/R 21% Inferior parietal lobule PFP, PF, PF L 16% Sec. somatosensory cortex OP4 L/R 11% Premotor cortex BA6 L/R	1, 4, 6, 8, 9, 10, 13, 14, 15, 16, 17, 18, 22, 23, 25, 27

Masked non-binary fCBP (functional connectivity based parcellation) enabled the distinction of spatial uniqueness (Tables 3A and 3B) and commonality (Table 3C) of independent components that form parcels. Analog to Tables 2A and 2B “unique voxels” (U) were left in the previous categorization in two types of “unique” voxels: Type previously “asymmetric and less connected” (Table 3A, highlighted in grey) and type previously “symmetric and connected” (Table 3B). An inverse laterality-index (L-I) was termed handedness-dependent (+), a concordant laterality-index meant handedness-independency (-). Common “voxels” were defined as voxels that overlapped in between parcels. To enable visualization of the “common” voxels, 9 groups of 2-6 spatially similar parcels (“common clusters”; C) were defined and correlated to whole brain RSN.

For a depiction of “unique” voxels please view Fig. 6A in [1], and for the “common clusters” view Fig. 6B in [1]. Each of the 30 parcels (P) was assigned to a separate color (cp. color scale Fig. 3 in [1]), which was also used for the parcel's “unique voxels”. The colors match between (left-handed) LH and right-handed (RH) subgroups. This color-code can also be seen in Table 3C, where each color represents one of the parcels included in the “common” cluster. U and C were anatomically characterized using the Harvard-Oxford structural cortical atlas in bold letters [6,7] and the Jülich histological (cyto- and myelo-architectonic) atlas in regular letters [8,9].

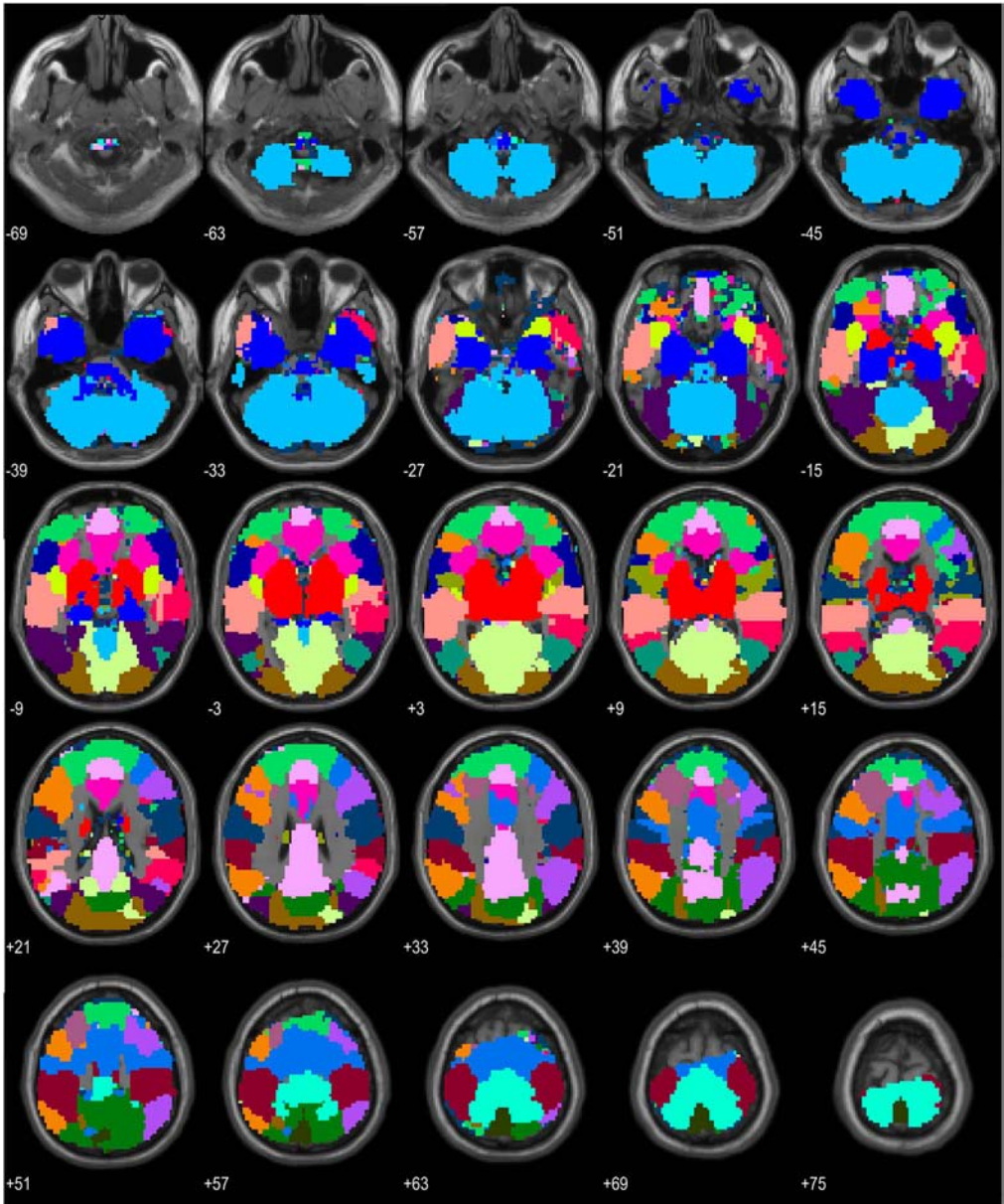


Fig. 1. Overlay of resulting 27 whole brain resting state networks (RSN). This overlay shows the spatial distribution of the 27 RSN systems. 80 dimensional whole brain ICA was performed on denoised fMRI data (LH and RH combined) using a whole brain mask. Each independent component (IC) was semi-automatically labeled to the 20 resting state network (RSN) atlas proposed by Laird et al. [4]. ICs that did not fit the Laird components (overall 7 of 80 or 8.75% of ICs) were checked visually and assigned to an anatomical label of the “Harvard-Oxford cortical structural atlas”. Here, sound behavioral interpretations to each IC (network) were determined by inserting their maximum xyz-MNI-coordinates in the large-scale, automated synthesis of human functional neuroimaging data platform Neurosynth (neurosynth.org), using a radius of 4 mm [5]. For an overview of these networks view Table 1. For an overview of the 80 dimensional whole brain ICA including their RSN attribution cp Fig. 2 in [1].

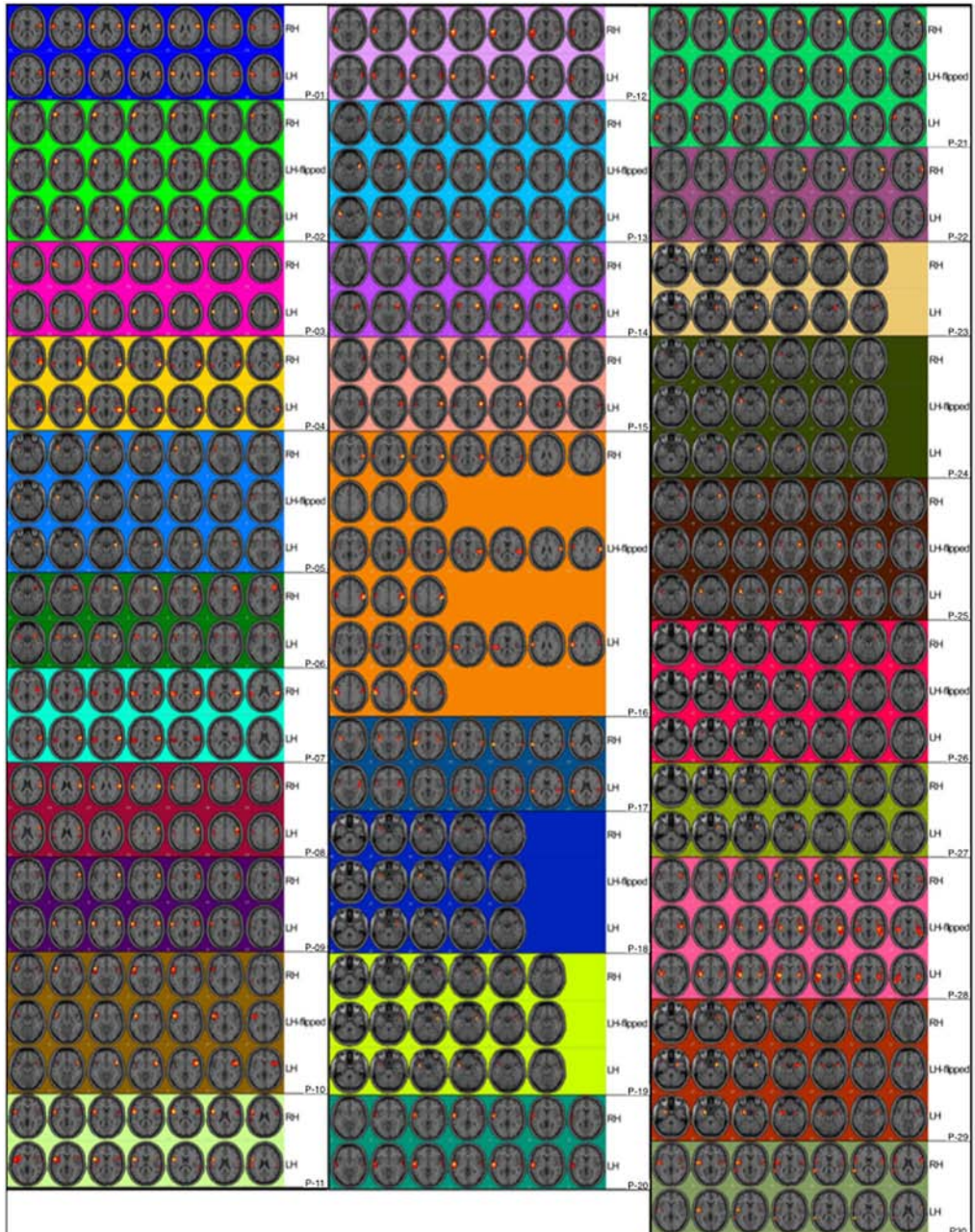


Fig. 2. Overview of 30 single parcels resulting from masked binary fCBP. To be able to compare LH and RH parcels we had to find analogous binary parcels between LH and RH. This approach was successful for interhemispheric symmetric parcels, but not for interhemispheric asymmetric parcels. Here, the parcels needed to be spatially flipped (mirrored) to correspond between LH and RH. This was done with respect to the x -axis, i.e. hemisphere-flip in x -direction in MNI-space. RH results are shown on the top row and the LH results in the lower row. Hemisphere-flips are depicted in the middle if necessary. The background colors represent the color of the parcel. The P number is indicated on the bottom right side of each overlap grouping. A more detailed depiction of spatially asymmetric and flipped parcels can be viewed in Fig. 4 of [1].

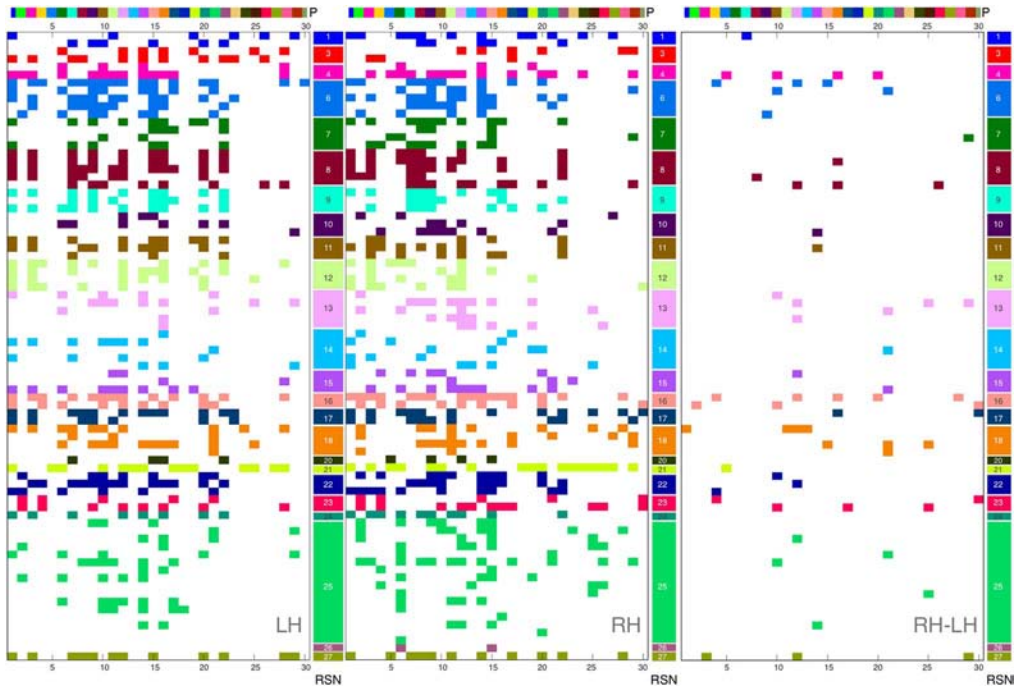


Fig. 3. P-to-RSN correlation matrix (FDR < 0.01). The x-axis (including colors) indicates the 30 parcels that resulted for LH and RH after masked binary fCBP (cp. Fig.3 in [1]). The third column represents differences between RH and LH. The y-axis (including colors) indicate the assignment to the 27 RSN systems as shown in Table 1. Note, that the number of RSN assignments to each parcel (P-to-RSN) did not differ between LH and RH. However, symmetrical parcels had significantly more RSN assignments than asymmetrical.

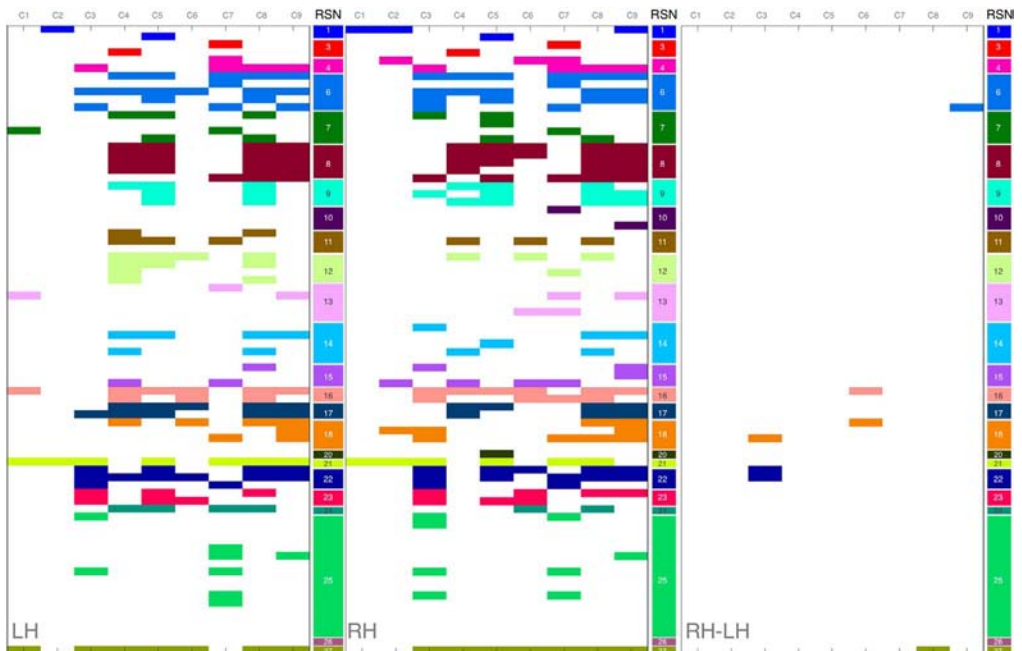


Fig. 4. C-to-RSN correlation matrix (FDR < 0.01). The x-axis indicates the 9 common clusters (C) that resulted for LH and RH after masked non-binary fCBP (cp. Fig. 6B in [1]). The third column represents differences between RH and LH. The y-axis (including colors) indicate the assignments of C to the 27 RSN systems as shown in Table 1. Please note, that apart from C1 “posterior insula” and C2 “inferior insula”, common clusters correlated with more than 5 RSN “systems”, which indicate manifold functionality.

Acknowledgements

Partially funded by the Society for the Advancement of Science and Research at the Medical Faculty of the Ludwig-Maximilians-Universität München (Verein zur Förderung von Wissenschaft und Forschung an der Medizinischen Fakultät der Ludwig-Maximilian Universität München), the Graduate School of Systemic Neurosciences (GSN), the German Foundation for Neurology (Deutsche Stiftung für Neurologie, DSN), the Hertie Foundation and the German Federal Ministry of Education and Research (German Center for Vertigo and Balance Disorders -IFB^{LMU}, Grant code 01EO140). This is a part of the dissertation of E. Kierig.

Transparency document. Supporting information

Transparency document associated with this article can be found in the online version at <https://doi.org/10.1016/j.dib.2019.01.014>.

References

- [1] V. Kirsch, R. Boegle, D. Keeser, E. Kierig, B. Ertl-Wagner, T. Brandt, M. Dieterich, Handedness-dependent functional organizational patterns within the bilateral vestibular cortical network revealed by fMRI connectivity based parcellation, *Neuroimage* 178 (2018) 224–237. <https://doi.org/10.1016/j.neuroimage.2018.05.018>.
- [2] C. Lopez, O. Blanke, F.W. Mast, The human vestibular cortex revealed by coordinate-based activation likelihood estimation meta-analysis, *Neuroscience* 212 (2012) 159–179. <https://doi.org/10.1016/j.neuroscience.2012.03.028>.
- [3] P. Zu Eulenburg, S. Caspers, C. Roski, S.B. Eickhoff, Meta-analytical definition and functional connectivity of the human vestibular cortex, *Neuroimage* 60 (2012) 162–169. <https://doi.org/10.1016/j.neuroimage.2011.12.032>.
- [4] A.R. Laird, P.M. Fox, S.B. Eickhoff, J.A. Turner, K.L. Ray, D.R. McKay, D.C. Glahn, C.F. Beckmann, S.M. Smith, P.T. Fox, Behavioral interpretations of intrinsic connectivity networks, *J. Cogn. Neurosci.* 23 (2011) 4022–4037. https://doi.org/10.1162/jocn_a_00077.
- [5] T. Yarkoni, R.A. Poldrack, T.E. Nichols, D.C. Van Essen, T.D. Wager, Large-scale automated synthesis of human functional neuroimaging data, *Nat. Methods* 8 (2011) 665–670. <https://doi.org/10.1038/nmeth.1635>.
- [6] R.S. Desikan, F. Ségonne, B. Fischl, B.T. Quinn, B.C. Dickerson, D. Blacker, R.L. Buckner, A.M. Dale, R.P. Maguire, B.T. Hyman, M. S. Albert, R.J. Killiany, An automated labeling system for subdividing the human cerebral cortex on MRI scans into gyral based regions of interest, *Neuroimage* 31 (2006) 968–980. <https://doi.org/10.1016/j.neuroimage.2006.01.021>.
- [7] N. Makris, J.M. Goldstein, D. Kennedy, S.M. Hodge, V.S. Caviness, S.V. Faraone, M.T. Tsuang, L.J. Seidman, Decreased volume of left and total anterior insular lobule in schizophrenia, *Schizophr. Res.* 83 (2006) 155–171. <https://doi.org/10.1016/j.schres.2005.11.020>.
- [8] S.B. Eickhoff, T. Paus, S. Caspers, M.H. Grosbras, A.C. Evans, K. Zilles, K. Amunts, Assignment of functional activations to probabilistic cytoarchitectonic areas revisited, *Neuroimage* 36 (2007) 511–521. <https://doi.org/10.1016/j.neuroimage.2007.03.060>.
- [9] S.B. Eickhoff, K.E. Stephan, H. Mohlberg, C. Grefkes, G.R. Fink, K. Amunts, K. Zilles, A new SPM toolbox for combining probabilistic cytoarchitectonic maps and functional imaging data, *Neuroimage* 25 (2005) 1325–1335. <https://doi.org/10.1016/j.neuroimage.2004.12.034>.